Int. J. Nano Dimens., 9 (2): 123-133, Spring 2018

ORIGINAL ARTICLE

The use of Gold nanorods conjugated with Herceptin in breast cancer treatment by photothermal therapy method in mouse model

Mohsen Kalantari[1]; Mojtaba Salouti[2,]; Kazem Parivar[1,*]; Mehrdad Hamidi[3]; Saeed Emadi[4]*

[1]*Department of Biology, Science and Research Branch, Islamic Azad University, Tehran, Iran*
[2]*Biology Research Center, Zanjan Branch, Islamic Azad University, Zanjan, Iran*
[3]*Zanjan Pharmaceutical Nanotechnology Research Center, Zanjan University of Medical Sciences, Zanjan, Iran*
[4]*Department of Biological Sciences, Institute for Advanced Studies in Basic Sciences (IASBS), Zanjan, Iran*

Received 27 September 2017; revised 18 December 2017; accepted 29 January 2018; available online 01 February 2018

Abstract

Treatment methods for breast cancer are not specific and each one has its own drawbacks. For this reason, scientists are seeking ways in which specifically affect cancer cells. Photothermal therapy is a method that uses near-infrared (NIR) laser energy to create sufficient heat to destroy cancer cells. In this study, the photothermal effect of gold nanorods (GNRs) was investigated for breast cancer treatment *in vitro* and *in vivo*. GNRs with the peak absorption of 808 nm were synthesized and conjugated with Herceptin (anti-HER2). After confirming the characteristics of the prepared conjugate, the therapeutic effect of the new agent was studied on SK-BR-3 cell line and BALB/c mouse model bearing breast tumor using the NIR laser. The cytotoxicity assay showed the biocompatibility of PEGylated GNRs-HER conjugate. Through the *in vitro* photothermal study, significant cell death was observed in breast cancer cells incubated with the conjugate along with the laser irradiation. Afterward, the biodistribution of the conjugate in the mouse model with breast tumor showed the considerable localization of new agent in breast tumor in comparison with other organs 24 h postinjection. The animal study showed a significant decrease in tumor growth rate as well as the increased lifespan of treated mice with breast tumor in comparison with the control groups.

Keywords: *Breast cancer; Gold nanorods; HER2 receptor; Herceptin; Photothermal therapy.*

How to cite this article

Kalantari M, Salouti M, Parivar K, Hamidi M, Emadi S. The use of Gold nanorods conjugated with Herceptin in breast cancer treatment by photothermal therapy method in mouse model. Int. J. Nano Dimens., 2018; 9 (2): 123-133.

INTRODUCTION

Breast cancer is a prominent cause of mortality in women worldwide [1-3]. Although surgery, chemotherapy, hormone therapy and radiation therapy can be successful, they have substantial disadvantages [4-6]. In recent years the application of nanoparticles for cancer therapy has found a great deal of interest [7, 8]. GNRs with their anisotropic shape exhibit two surface plasmon resonances: one is transverse and the other is the longitudinal that can be converted from the visible to the near-infrared (NIR) region by controlling the aspect ratio of the rods [9]. The use of GNRs in near-infrared plasmonic photothermal therapy is an interesting approach due to their rapid fabrication and bioconjugation, tunable optical absorption and strong surface plasmon resonance in NIR region [10-12]. GNRs are capable of converting NIR laser light into the thermal heat [2]. Strong optical absorption and the heat generation from GNRs can be utilized in cancer therapy to destroy cancerous cells [13].

Active targeting enhances the GNRs localization within the tumor by attachment of a targeting moiety over-expressed in cancer cells [14]. Monoclonal antibodies are classic tools to target tumor markers such as HER2 on the surface of cancer cells. HER2 regulate cell growth, differentiation, and survival. Overexpression of HER2 gene occurs in 20-25% of breast tumors. The number of receptors can increase 40-fold in

* Corresponding Author Email: saloutim@yahoo.com
kazem_parivar@yahoo.com

tumors. Trastuzumab (Herceptin), a recombinant humanized monoclonal antibody, targets the extracellular domain of the transmembrane HER2 and is used in the treatment of HER2-positive breast cancer [15-18]. Active targeting requires successful conjugation of GNRs to the antibody using covalent bonds to ensure specific delivery to the tumor [19]. El-Sayed *et al.* in 2006 reported the killing effect of gold nanoparticles of spherical shape conjugated with anti-EGFR and laser light on epithelial cancer cells *in vitro*. [20]. At the same year, Huang *et al.* studied the effect of GNRs conjugated with anti-EGFR using NIR light on the malignant oral cancer cells *in vitro*. They found that the malignant cells require about half the laser energy to be destroyed then the normal cells after exposure to the continuous red laser at 800 nm [21]. Eghtedari *et al.* in 2008 described a novel technique for functionalizing GNRs by covalent attachment of Herceptin (HER) to image the breast cancer in athymic nude mice. They demonstrated significant accumulation of GNRs within breast tumor [22]. Heidari *et al*. in 2015, used photothermal method successfully for the killing of breast cancer cells using bombesin peptide conjugated with GNRs [10]. There is not any published work about the photothermal therapy of breast tumor using Herceptin conjugated with GNRs in the animal model as far as we know. In this research, we constructed a novel complex, GNRs-HER, PEGylated with poly(ethylene glycol) to enhance the biocompatibility, then the therapeutic effect of targeted GNRs was investigated on breast tumor using plasmonic photothermal therapy as a non-invasive method.

EXPERIMENTAL

Materials

Cetrimonium bromide (CTAB), Chlorid trihydrate ($HAuCl_4.3H_2O$), ascorbic acid, trypan blue, nitric acid, hydrochloric acid, N-Hydroxcysulfosuccinimide (sulfo-NHS), Nanothinks ACID16 (or16-Mercaptohexadecanoic acid), EDC (*N*-[3-Dimethylaminopropyl]-*N'*-ethylcarbodiimide) and MTT (Methylthiazolyldiphenyl-tetrazolium bromide) were purchased from Sigma-Aldrich. Silver nitrate ($AgNO_3$) and sodium borohydride ($NaBH_4$) were purchased from Merck, Germany. mPEG-SH (5000 Da) was purchased from Nanocs, USA. RPMI 1640 medium, DMEM medium, FBS (Fetal Bovine Serum), Pen-Strep solution and Trypsin-EDTA, Phenol red solution (0.25%) were purchased from Gibco (USA). Trastuzumab (Herceptin) was purchased from Roche Company (USA). All glassware was cleaned with aqua regia (HCl/HNO_3) and rinsed twice with deionized water before using.

Cell lines and culture conditions

SK-BR-3 cells (a human breast adenocarcinoma cell line overexpressing HER2 receptors), purchased from Iranian Biological Resource Center, Tehran and Iran were cultured in DMEM. T47D cells (a human breast cancer cell line not expressing HER2 receptors) and 4T1 cells, a mouse breast cancer cell line purchased from Pasteur Institute, Tehran, Iran, were cultured in RPMI-1640 supplemented with 1% Pen-Strep and 10% FBS. The cells were incubated in a humidified incubator containing 5% CO_2 at 37 °C.

Synthesis and Characterization of GNRs

GNRs with a peak absorption wavelength of 808 nm were produced according to the seed-mediated growth procedure reported by Eghtedari *et al.* in 2008 [22]. Briefly, a gold seed solution was prepared by the addition of 7.5 ml of 0.1 M CTAB to 250 µl of 0.01 M gold chloride. Then, 600 µl of 0.01 M $NaBH_4$ in ice-cold DI water was quickly added in the uncapped tube (as it may release some gases) and kept the seed solution at 30°C to prevent crystal formation. Then, 4.7 ml of 0.1 M CTAB, 200 µl of 0.01 M gold chloride and 40 µl of 0.01 M $AgNO_3$ were mixed together in three 15 ml tubes to prepare the growth solution. The solution color was yellow/brown at the beginning but it became translucent upon the addition of 32 µl of 0.1 M ascorbic acid. Then, the seed solution (21 µl) was added to the unstirred growth solution and allowed to react at 30 °C for 1 h. The solution color was changed to purple/brownish. Transmission electron microscopy (TEM) was used to find the size and morphology of the synthesized nanoparticles using a PHILIPS EM 208 TEM. Then, the nanoparticles were characterized by UV-vis spectroscopy. Measurements were made in triplicate for each sample [23, 24].

GNRs Biofunctionalization, Conjugation to Antibody and PEGylation

5 ml of GNRs solution (in CTAB) were centrifuged twice at 9000 rpm for 20 min and redispersed in DI water to remove excess CTAB molecules. To prevent aggregation, 50 µl of 5 mM

Nanothinks ACID16 (MHDA) was added to the GNRs solution and sonicated for 16 min at 55 °C, the temperature was decreased to 28 °C while sonication was continued for 2 h. The solution was centrifuged at 9000 rpm for 15 min, and the pellet was resuspended in phosphate buffer saline (PBS). Then, 50 µl EDC (10 mM) and sulfo-NHS (0.4 mM) were added to the solution. The activated GNRs were produced by sonicating the mixture for 30 min at 4°C. Then, Herceptin (21 $mg.ml^{-1}$) was added to 5 ml of the GNRs and sonicated at room temperature for 120 min. Following the removal of excess Herceptin by centrifugation, 50 µl of PEG-thiol (5000 D molecular weight)) with the concentration of 10 mM was added to the mixture to increase the blood circulation time of nanoparticles and the mixture was incubated at room temperature for 10 h. The solution of GNRs-HER-PEG conjugate was centrifuged at 9000 rpm for 15 min, and re-dispersed in PBS to remove unbound PEG molecules [11, 25, 26]. The Fig. 1 illustrates the conjugation process.

Bioconjugation Confirmation

The characteristics of the new conjugate were checked by two procedures. The absorption spectrum was obtained using a UV/Vis spectrophotometer (UV-Vis-NIR spectrometry, c0r10 model, Takfam Sazan Teif Noor, IRAN) for investigating the interaction of Herceptin with GNRs. The spectroscopy was performed in the range of 400 to 900 nm at the resolution of 1 nm. Fourier transform infrared spectroscopy (FT/IR-6300, Jasco, USA) was performed to evaluate the binding of GNRs with Herceptin. The recorded IR spectra of Herceptin, GNRs, and GNRs- Herceptin conjugate were between 400 and 4000 cm^{-1} [23, 27].

Optical Stability

GNRs-HER-PEG conjugate 0.02l M GNRs concentration) was added to the mixture of human blood serum and PBS (2:1) and the optical absorbance was measured at 808 nm after one overnight. The control solution was included human blood serum and PBS only (2/1 ratio). The absorbance of GNRs-PEG-HER conjugate was determined by subtracting the ‘‘serum’’ absorbance from ‘‘the conjugate in serum’’ absorbance [27, 28].

Cell Toxicity Assessment

The MTT assay was used to evaluate the possible cytotoxicity of the prepared conjugate. The level of MTT cleavage by viable cells was studied by the absorbance of formazan at 630 nm using an ELISA plate reader. SK-BR-3 cell line was cultured at 5000 cells per well in a 96-well microplate with a 100 µl DMEM medium and incubated at 37°C one overnight in a 5% CO_2. Then, the cell plates were washed with PBS and 100 µl of culture medium with the appropriate concentration of samples including PEG-GNRs, GNRs-CTAB, and GNRs-HER-PEG were added to each well and incubated one overnight. Then, 10 µl of MTT dissolved in PBS (5 mg/ml) was added to each well and incubated for 4 h. Finally, 100 µl of dimethyl sulfoxide (DMSO) was added to each well and the quantity of formazan was measured by optical absorbance at the wavelength of 630 nm.

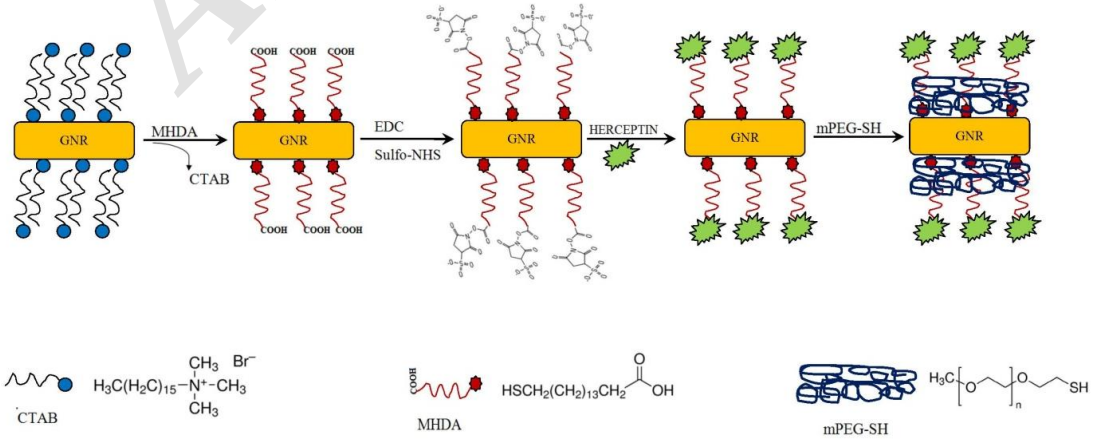

Fig .1: Schematic representation of the conjugation of GNRs with Herceptin and the PEGylation process.

The percentage of survival compared with the untreated cells (control) was expressed as the cell viability [29, 30].

Binding Study

The specific binding of GNRs-HER-PEG conjugate to overexpressing HER2 receptor cancer cells (SK-BR-3 cell line) was examined using the binding assay method. T47D cell line (not expressing HER2) was used as the control cells. The SK-BR-3 cells and T47D cells were cultured in DMEM and RPMI-1640, respectively. GNRs-HER-PEG conjugate (as the active targeting agent) and GNRs-PEG (as the passive targeting agent) with a concentration of 0.02 µM ml^{-1} were added to the cell plates and incubated at 37 °C with 5% CO_2 for 60 min. PBS was used to wash the cell plates for removing the unattached GNRs-HER-PEG molecules. The cells were observed by an inverted microscope (Model IX70) [23, 28].

In vitro Near-infrared Photothermal Therapy

SK-BR-3 and T47D cells were cultured in a 96-well plate at a density of 5000 cells/well, and incubated overnight for cell adhesion. The medium was replaced with fresh medium containing the GNRs-CTAB, GNRs-HER-PEG, and PBS alone. After 1 h incubation, the cells were washed 3 times with PBS to remove unbound particles. Then, the cells were irradiated by NIR laser at 808 nm with a power of 80 mW for 3 min. The cells were incubated with MTT (0.5 mg ml^{-1}) in a medium in dark for 4 h and mixed with 100 µl DMSO after the supernatant was removed. The optical density was measured at 630 nm using a microplate reader (Starfox-2100, Awareness, USA). The percentage of OD value of the main group over the control group was considered as the cell viability [31, 32].

Tumor Model

Inbred BALB/c mice of 5 to 8 weeks old were purchased from Pasteur Institute, Karaj, Iran and housed in our animal research facility in accordance with free access to food and water. For solid tumor induction in the mouse model, 4T1 cells were inoculated subcutaneously with 5×10^5 viable cells into the left side of abdominal region (between leg and hand) of the mice. Animals were used in experiments on days 12 to 14 after the inoculation of cells when tumor volume was approximately 0.5 cm^3. All the animal studies were confirmed by Animal Care Committee of Tarbiat Modares University, Tehran, Iran.

Biodistribution Study

After the tumors had reached a proper size in the mice, the biodistribution of GNRs-HER-PEG conjugate in blood, vital organs and tumor was studied. 200 µl of GNRs-HER-PEG were injected via the tail vein (5 mice for each time points). The mice were sacrificed by CO_2 gas suffocation at 6, 12 and 24 h time points, major organs and tumor were dissected, weighed and dissolved by adding 10 ml of HCl and 4 ml of HNO_3 at 75°C for 40 min and filtered with 0.45 µm Teflon filter. After evaporating the solution, a few ml of 0.5 N hydrochloric acid was added and the sample was monitored for GNRs using an atomic absorption spectrophotometer (VARIAN, model AA240FS). The uptake of GNRs-HER-PEG conjugate in each organ was determined as a mean percentage of injected doses per gram of organ tissues (%ID/g) [23, 33].

In vivo Near-infrared Photothermal Therapy

Through a subcutaneous injection of 5×10^5 cells suspended in the flank region, the mice bearing 4T1 tumor were successfully established. After two weeks, 25 mice with similar tumor sizes were separated into five groups including GNRs-HER-PEG conjugates plus laser, GNRs-HER-PEG conjugate alone, Herceptin alone, laser alone and PBS alone (control). 100 µl of each trial solution was injected via the tail vein of the mice. The tumor region was irradiated with 808 nm continuous-wave laser with a power of 80 mW for 10 min (just in laser plus groups) 24 h after the injection. The tumor morphology was recorded with a digital color camera during the treatment and the tumor size was measured using a caliper every day. The formula: $V=L\times W^2/2$ was used to measure the tumor volume. In this equation, V, L and W are tumor volume, length, and width, respectively. The relative tumor volume was calculated *as V/V0* (*V* is the tumor volume at the day of measuring and V0 is the tumor volume when the treatment was initiated). In addition, the effect of treatment on the survival time of treated mice was studied in all the groups too [34-36].

Statistical Analysis

The results were analyzed in SPSS (version 16.0) by analysis of variance (ANOVA) and Fisher's least significant difference (LSD) test. P-value < 0.05 was considered statistically significant. All the experiments were repeated 3 times.

RESULTS AND DISCUSSION

Characterization of Synthesized GNRs

The TEM image showed that the synthesized GNRs were approximately 11 nm in width and 42 nm length (3.9 aspect ratio), with a longitudinal plasmon absorption maximum around 808 nm. According to the study performed by UV/Vis spectroscopy, the synthesized GNRs had two SPR wavelengths: A higher wavelength band near 808 nm, and a lower wavelength band near 520 nm. Fig. 2a shows the absorption spectrum and Fig. 2b shows TEM image of the produced GNRs.

Characterization of GNRs-HER Conjugate

The successful conjugation of GNRs with Herceptin was approved by UV–Vis and FTIR spectroscopies. As seen in Fig. 3, the spectrum of GNRs shows a 6 nm shift in the SPR peak after binding GNRs to Herceptin. The shift may be due to the altered refractive index of the nanoparticles environment caused by the presence of biological molecules. A redshift of 5 nm was found in the absorbance peaks between the GNRs-HER and GNRs-HER-PEG conjugates too. The shift demonstrates successful binding of PEG molecules to GNRs surfaces. No broadening in the plasmon band after binding of Herceptin to GNRs shows no aggregation of GNRs during the process. Fig. 4 illustrates the FTIR spectra of MHDA and GNRs-MHDA-HER conjugate. The peak at 1730 cm^{-1} is related to the C=O stretching frequency of the carboxylic acid group of the MHDA molecule (Fig. 4a). After the conjugation process, and binding of Herceptin amino group to the carboxyl group of MHDA, the appearance of the characteristic peaks of the monosubstituted (secondary) amides, R-CO-NH-R, carbonyl stretching of amide I band at 1640 cm^{-1} demonstrated that Herceptin amine groups and MHDA carboxyl groups successfully have connected to each other and formed the amide bond (Fig. 4b).

Stability

The new conjugate must remain intact in blood sufficiently enough time after injection to be accumulated at the tumor site. The optical absorbance of GNRs-HER-PEG conjugate and blood serum plus conjugate were studied at 808 nm after 24 h incubation. As it can be seen in Fig. 5, widening of the longitudinal plasmon resonance band is not observed. This finding demonstrated the high stability of the new agent in blood serum.

Cell toxicity

The toxicity of the GNRs-HER-PEG conjugate, GNR-PEG, and GNRs alone was assessed using the MTT assay. Fig. 6 demonstrates cell viability of SK-BR-3 cells after incubation with the prepared conjugate for 24 h (within the GNRs concentration of 20 µg ml^{-1}). GNRs exhibited high cytotoxicity against the treated cells, indicating that they were highly toxic due to the presence of CTAB. The GNRs-HER-PEG and GNR-PEG showed little or no toxicity at the same concentration (almost 94% and 96% viability, respectively; $P < 0.05$). These results confirm that our fabricated conjugate is well-tolerated by the normal cells.

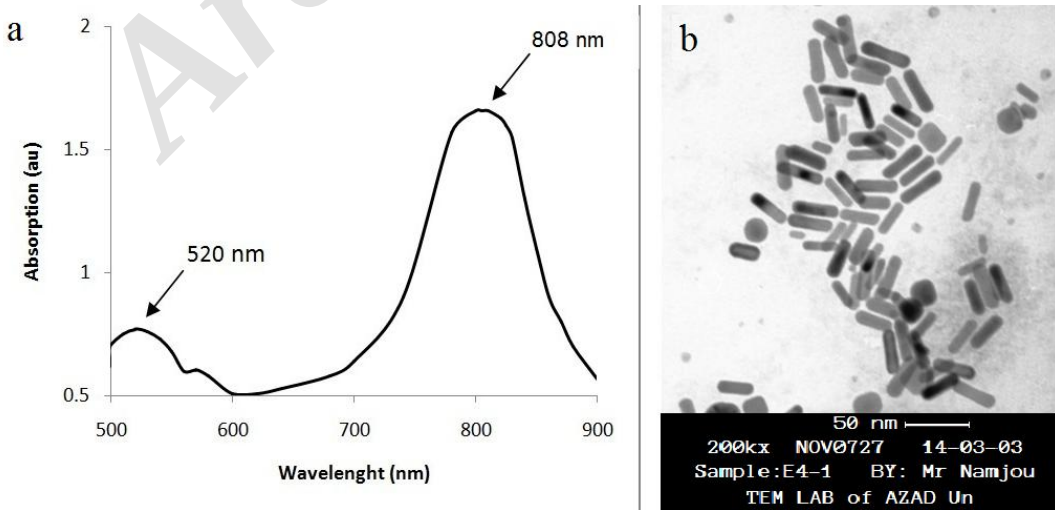

Fig. 2: a) UV–vis spectrum of synthesized GNRs using the seed-mediated growth method. b) TEM image of GNRs.

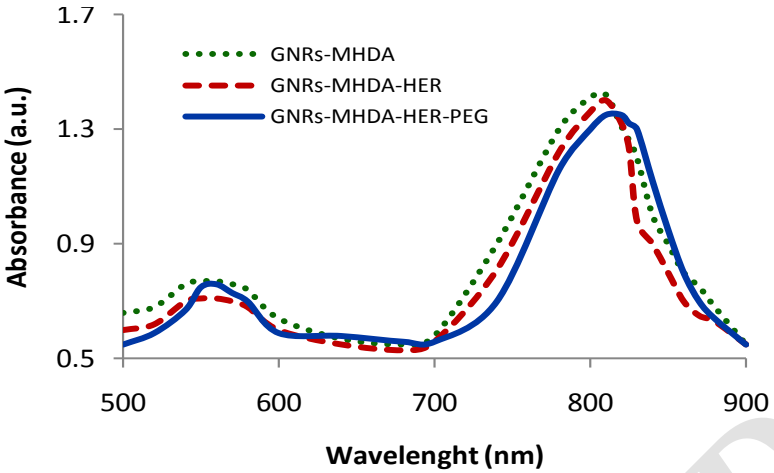

Fig. 3: UV/vis spectra of GNRs-MHDA, GNR-MHDA-HER and GNR-MHDA-HER-PEG conjugate. The red shifting after each step indicates the successful fabrication of GNRs.

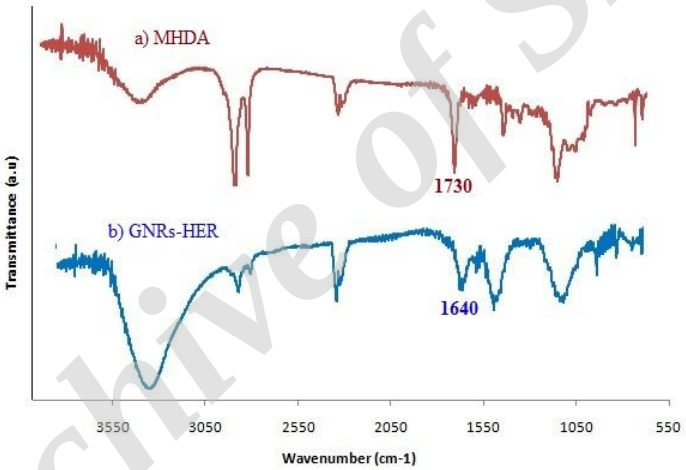

Fig. 4: FT-IR spectra: a) MHDA and b) GNR-MHDA-HER.

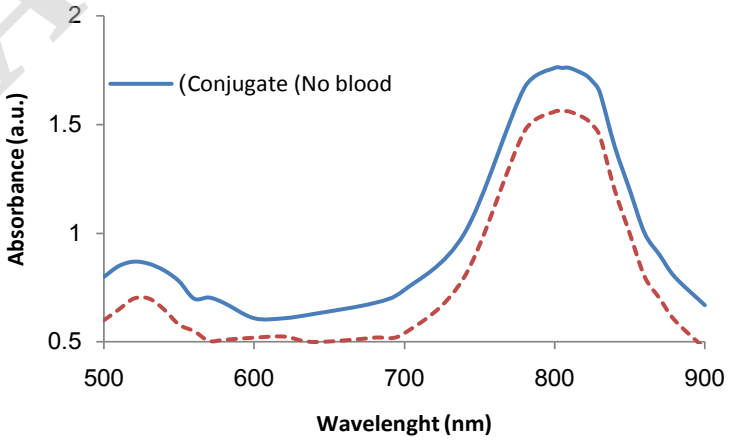

Fig. 5: Optical serum stability. The GNRs-HER-PEG showed a high level of optical stability after incubation in human serum for 24 h.

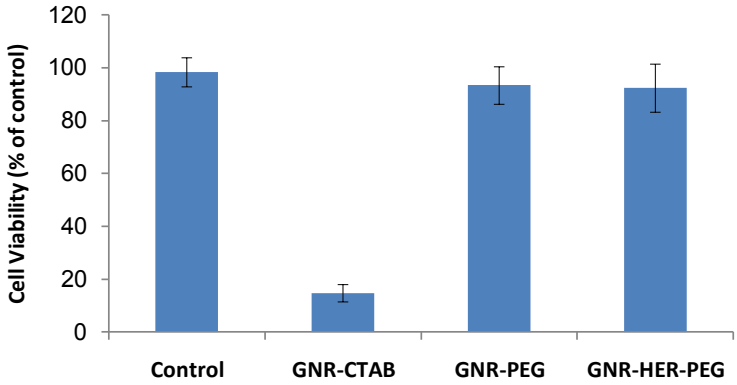

Fig. 6: Cell viability of SK-BR-3 cells after incubation with GNRs-HER-PEG, GNR-PEG and GNR alone for 24h.

Binding Study

The dark spots bonded to the surface of SK-BR-3 cells shows the selective binding of the GNRs-HER-PEG conjugate to the cells (Fig. 7a). The SK-BR-3 cells were labeled with the new agent due to the specific binding of Herceptin to the overexpressed HER2 receptors in comparison with T47D cells, not expressing HER2 receptors (Fig. 7b). This finding proves the specific interaction of the new agent with breast cancer cells.

Photothermal Therapy In vitro using GNRs-HER-PEG Conjugate

We used MTT assay investigate the effects of GNRs-HER-PEG conjugate on SK-BR-3 and T47D cells during laser treatment. As seen from Fig. 8, after the photothermal treatment, about 30% of SK-BR-3 cells exposed to the prepared conjugate plus NIR laser irradiation were dead; while T47D cells and the other groups (GNRs-HER-PEG without the laser, laser alone, and control groups) demonstrated no considerable damages to the cancer cells. There were seen a large number of cell death in both cell lines treated with GNRs due to the high toxicity of CTAB.

Biodistribution Study

Biodistribution of GNRs-HER-PEG conjugate was performed using BALB/c mice bearing breast tumor at 6, 12, and 24 h after intravenous injection. As shown in the Fig. 9, the uptake of conjugate in the tumor tissue increases as time passes. After 24 h post-injection, the percentage of the conjugate in the tumor was reached to maximum (~9% injected dose/gram) which approved the capability of the conjugate to target the breast tumor. So, 24 h post-injection was fixed as the best time for NIR laser irradiation on the tumor location in the animal study (p-value <0.05). It was also observed that almost 7% of the conjugate was uptaken by the liver due the reticuloendothelial system (RES).

In vivo Photothermal Therapy

After confirming the photothermal outcome *in vitro*, the *in vivo* photothermal treatment study was performed. For this purpose, the mice bearing 4T1 tumor were divided randomly into five treatment groups (n=5).

After two weeks when the tumor volume was approximately 0.5 cm^3, the tumor size and animal survival were monitored for 21 days following the beginning of treatments. As shown in Fig. 10, the tumor growth was significantly suppressed after the mice treated with GNRs-HER-PEG conjugate followed by laser irradiation at the wavelength of 808 nm. Meanwhile, the tumor size in Herceptin alone, laser alone and the conjugate without laser and control groups continued to grow rapidly (p-value<0.05).

The effect of treatment on survival of the mice in different groups was studied too. The survival of the photothermally treated group was longer (approximately 86%) than the control group. The control mice died after 20 ± 3 days on average while the mice treated with GNRs-HER-PEG, died at the day 37 ± 4 after treatment on average (Fig. 11).

Representative photos of mice bearing 4T1 tumors after treatment with GNRs-HER-PEG plus laser (Fig. 12a) indicated that the growth of the tumor is suppressed significantly in comparison with control group (Fig. 12b). These results clearly showed evidence of tumor growth inhibition by the photothermal therapy method using GNRs-HER-PEG conjugate.

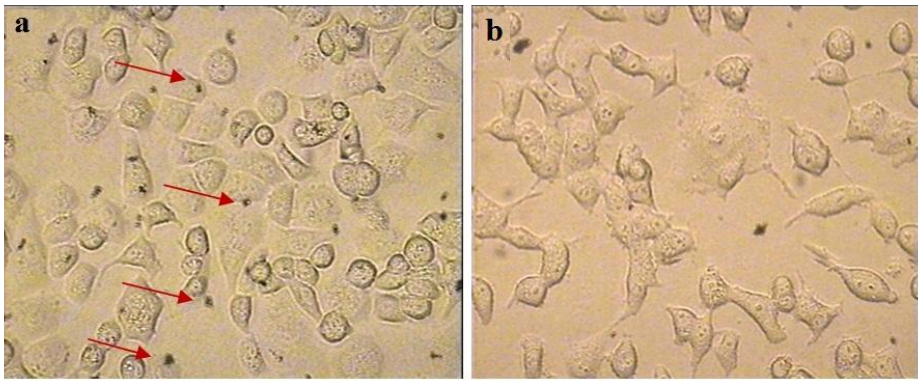

Fig. 7: Selective binding study. a) SK-BR-3 incubated with GNRs-HER-PEG. The dark spots can be seen attached to the cells. A number of specific binding was shown with arrows. b) T47D cells incubated with GNRs-HER-PEG. For these cells, specific binding was not observed (Total magnification is 200X).

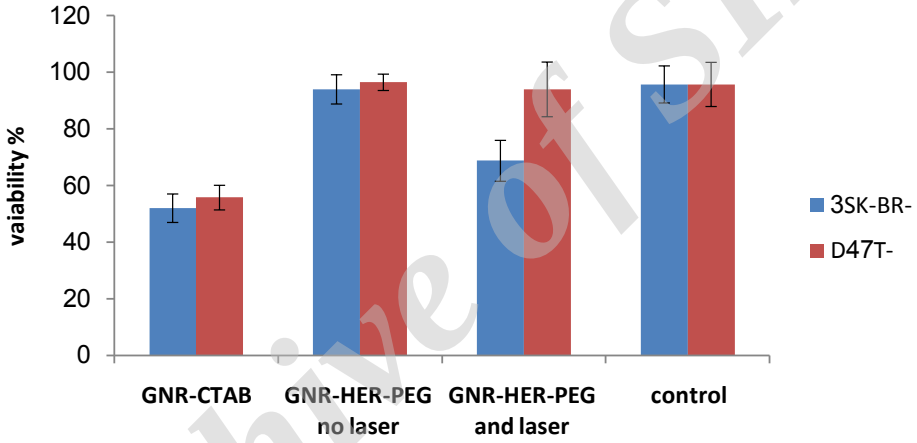

Fig. 8: The viability percentage of SK-BR-3 and T47D cells after incubation with GNRs-HER-PEG conjugate and being irradiated with 808 nm laser (p-value < 0.05).

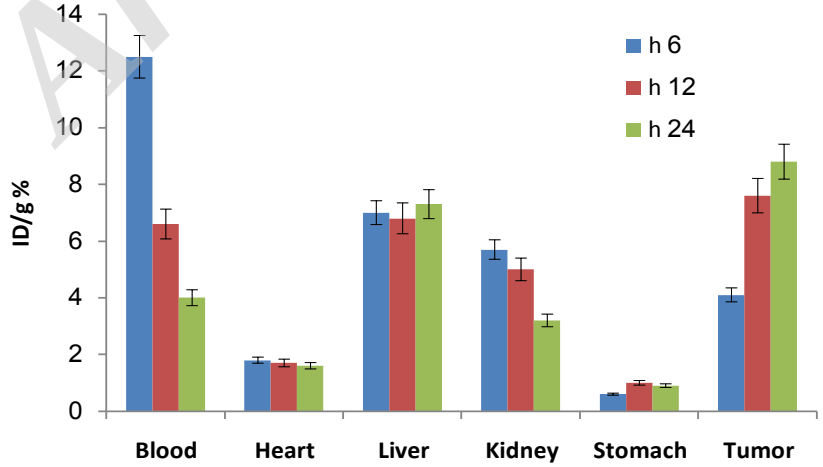

Fig. 9: Biodistribution data of GNRs-HER-PEG in BALB/c mice bearing breast tumor in blood, vital organs and tumor at different time post injection, measured by atomic adsorption spectroscopy (n=5).

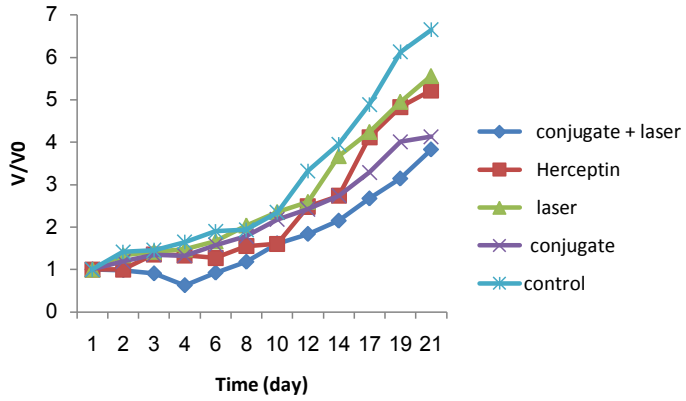

Fig. 10: Tumor volume measurement at several time points in different mice groups after the treatment (A). The tumor volumes in different groups were normalized to their initial sizes. Laser wavelength =808 nm; power density =80 mW; irradiation time =10 min. There was no statistical difference among groups in tumors volumes at the onset of treatment.

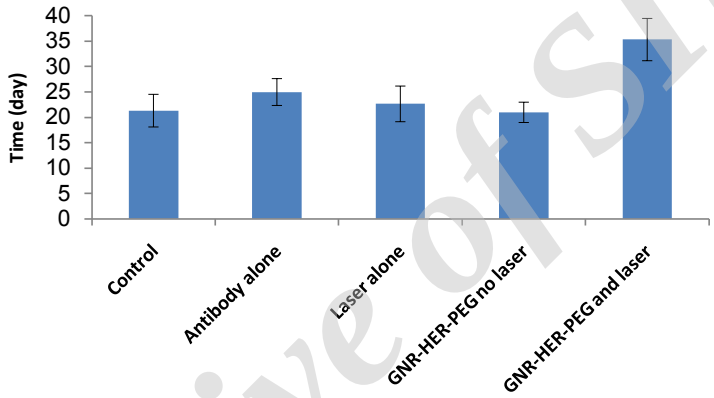

Fig. 11: The mean survival time of the mice treated with GNRs-HER-PEG plus laser was significantly higher than control groups (p-value <0.05).

Fig. 12: *In vivo* photothermal therapy. The photos show two representative mice bearing 4T1 tumors treated with GNRs-HER-PEG plus laser (Fig. 12a) and PBS only as a control (Fig. 12b). The photos illustrate the success of the prepared conjugate as a photothermal agent to inhibit the growth of tumor in comparison with the control mouse.

CONCLUSION

In summary, the present study reports the successful fabrication of GNRs-HER-PEG conjugate offering targeting capability to track and attach to the breast cancer cells. The results clearly showed the evidence of tumor growth inhibition by the prepared photothermal agent significantly in the mouse model.

CONFLICT OF INTEREST

The authors declare that there is no conflict of interests regarding the publication of this manuscript.

REFERENCES

[1] DeSantis C. E., Fedewa S. A., Goding Sauer A., Kramer J. L., Smith R. A., Jemal A., (2016), Breast cancer statistics, 2015: Convergence of incidence rates between black and white women. *CA: A Cancer J. Clinicians*. 66: 31-42.

[2] Abdoon A. S., Al-Ashkar E. A., Kandil O. M., Shaban A. M., Khaled H. M., El Sayed M. A., Hussein H. A., (2016), Efficacy and toxicity of plasmonic photothermal therapy (PPTT) using gold nanorods (GNRs) against mammary tumors in dogs and cats. *Nanomedicine: Nanotechnol., Biology and Medicine*. 12: 2291-2297.

[3] Srinivas P., Mounika G., (2011), Nanomedicine: The role of newer drug delivery technologies in cancer. *Int. J. Nano Dimens.* 2: 1-15.

[4] Huang X., El-Sayed M. A., (2011), Plasmonic photo-thermal therapy (PPTT). *Alexandria J. Medic.* 47: 1-9.

[5] Ahmad R., Fu J., He N., Li S., (2016), Advanced gold nanomaterials for photothermal therapy of cancer. *J. Nanosci. Nanotechnol.* 16: 67-80.

[6] Marsh M., Schelew E., Wolf S., Skippon T., (2009), Gold nanoparticles for cancer treatment. *Queen's Univ. Kingston*. *29*.

[7] Wang J., Sui M., Fan W., (2010), Nanoparticles for tumor targeted therapies and their pharmacokinetics. *Current Drug Metabol.* 11: 129-141.

[8] Praetorius N. P., Mandal T. K., (2007), Engineered nanoparticles in cancer therapy. *Recent Patents on Drug Del. Formul.* 1: 37-51.

[9] Hwang S., Nam J., Jung S., Song J., Doh H., Kim S., (2014), Gold nanoparticle-mediated photothermal therapy: Current status and future perspective. *Nanomedic.* 9: 2003-2022.

[10] Heidari Z., Salouti M., Sariri R., (2015), Breast cancer photothermal therapy based on gold nanorods targeted by covalently-coupled bombesin peptide. *Nanotechnol.* 26: 195101-195108.

[11] Dickerson E. B., Dreaden E. C., Huang X., El-Sayed I. H., Chu H., Pushpanketh S., El-Sayed M. A., (2008), Gold nanorod assisted near-infrared plasmonic photothermal therapy (PPTT) of squamous cell carcinoma in mice. *Cancer let.* 269: 57-66.

[12] Huang X., El-Sayed M. A., (2010), Gold nanoparticles: Optical properties and implementations in cancer diagnosis and photothermal therapy. *J. Adv. Res.* 1: 13-28.

[13] Abadeer N. S., Murphy C. J., (2016), Recent progress in cancer thermal therapy using gold nanoparticles. *J. Phys. Chem. C*. 120: 4691-4716.

[14] Singh M., Harris-Birtill D. C., Markar S. R., Hanna G. B., Elson D. S., (2015), Application of gold nanoparticles for gastrointestinal cancer theranostics: A systematic review. *Nanomedicine: Nanotechnol., Biology and Medic.* 11: 2083-2098.

[15] Tolaney S. M., Krop I. E., (2009), Mechanisms of trastuzumab resistance in breast cancer. *Anti-Canc. Agents in Medic. Chem. (Formerly Current Medicinal Chemistry-Anti-Cancer Agents)*. 9: 348-355.

[16] Daniele L., Sapino A., (2009), Anti-HER2 treatment and breast cancer: State of the art, recent patents, and new strategies. *Recent Patents on Anti-Canc. Drug Discov*. 4: 9-18.

[17] Leveque D., Gigou L., Bergerat J. P., (2008), Clinical pharmacology of trastuzumab. *Current Clinical Pharmacol.* 3: 51-55.

[18] Widakowich C., Dinh P., Azambuja E. D., Awada A., Piccart-Gebhart M., (2008), HER-2 positive breast cancer: What else beyond trastuzumab-based therapy?. *Anti-Cancer Agents in Medic. Chem. (Formerly Current Medicinal Chemistry-Anti-Cancer Agents)*. 8: 488-496.

[19] Green H. N., Martyshkin D. V., Rodenburg C. M., Rosenthal E. L., Mirov S. B., (2011), Gold nanorod bioconjugates for active tumor targeting and photothermal therapy. *J. Nanotechnol.* 2011: Article ID 631753, 7 pages.

[20] El-Sayed I. H., Huang X., El-Sayed M. A., (2006), Selective laser photo-thermal therapy of epithelial carcinoma using anti-EGFR antibody conjugated gold nanoparticles. *Cancer Lett.* 239: 129-135.

[21] Huang X., El-Sayed I. H., Qian W., El-Sayed M. A., (2006), Cancer cell imaging and photothermal therapy in the near-infrared region by using gold nanorods. *J. Am. Chem. Soc.* 128: 2115-2120.

[22] Eghtedari M., Liopo A. V., Copland J. A., Oraevsky A. A., Motamedi M., (2008), Engineering of hetero-functional gold nanorods for the in vivo molecular targeting of breast cancer cells. *Nano Lett.* 9: 287-291.

[23] Heidari Z., Sariri R., Salouti M., (2014), Gold nanorods-bombesin conjugate as a potential targeted imaging agent for detection of breast cancer. *J. Photochem. Photobio. B: Biology*. 130: 40-46.

[24] Almaki J. H., Nasiri R., Idris A., Majid F. A. A., Salouti M., Wong T. S., Amini N., (2016), Synthesis, characterization and in vitro evaluation of exquisite targeting SPIONs–PEG–HER in HER^{2+} human breast cancer cells. *Nanotechnol.* 27: 105601-105608.

[25] Liopo A., Conjusteau A., Oraevsky A., (2012), PEG-coated gold nanorod monoclonal antibody conjugates in preclinical research with optoacoustic tomography, photothermal therapy and sensing. *Proc. SPIE*. 8223: 822344-822349.

[26] Wang Y., Black K. C., Luehmann H., Li W., Zhang Y., Cai X., Li Z. Y., (2013), Comparison study of gold nanohexapods, nanorods, and nanocages for photothermal cancer treatment. *ACS Nano*. 7: 2068-2077.

[27] Jafari A., Salouti M., Shayesteh S. F., Heidari Z., Rajabi A. B., Boustani K., Nahardani A., (2015), Synthesis and characterization of Bombesin-superparamagnetic iron oxide nanoparticles as a targeted contrast agent for imaging of breast cancer using MRI. *Nanotechnol.* 26: 075101-075107.

[28] Lu J., Owen S. C., Shoichet M. S., (2011), Stability of self-assembled polymeric micelles in serum. *Macromolec.* 44: 6002-6008.

[29] Zhou F., Xing D., Ou Z., Wu B., Resasco D. E., Chen W. R.,

(2009), Cancer photothermal therapy in the near-infrared region by using single-walled carbon nanotubes. *J. Biomed. Optic.* 14: 021009-021009.

[30] Hoffmann J., Bohlmann R., Heinrich N., Hofmeister H., Kroll J., Künzer H., Gieschen H., (2004), Characterization of new estrogen receptor destabilizing compounds: Effects on estrogen-sensitive and tamoxifen-resistant breast cancer. *J. National Cancer Ins.* 96: 210-218.

[31] Shen S., Tang H., Zhang X., Ren J., Pang Z., Wang D., Yang W., (2013), Targeting mesoporous silica-encapsulated gold nanorods for chemo-photothermal therapy with near-infrared radiation. *Biomater:* 34: 3150-3158.

[32] Zhu H., Chen Y., Yan F. J., Chen J., Tao X. F., Ling J., Mao Z. W., (2017), Polysarcosine brush stabilized gold nanorods for in vivo near-infrared photothermal tumor therapy. *Acta biomaterialia*. 50: 534-545.

[33] Liu Z., Cai W., He L., Nakayama N., Chen K., Sun X., Dai H., (2007), In vivo biodistribution and highly efficient tumour targeting of carbon nanotubes in mice. *Nature Nanotechnol.* 2: 47-52.

[34] Yang M., Liu Y., Hou W., Zhi X., Zhang C., Jiang X., Cui D., (2017), Mitomycin C-treated human-induced pluripotent stem cells as a safe delivery system of gold nanorods for targeted photothermal therapy of gastric cancer. *Nanoscale*. 9: 334-340.

[35] Chu M., Shao Y., Peng J., Dai X., Li H., Wu Q., Shi D., (2013), Near-infrared laser light mediated cancer therapy by photothermal effect of Fe_3O_4 magnetic nanoparticles. *Biomater.* 34: 4078-4088.

[36] Shen S., Wang S., Zheng R., Zhu X., Jiang X., Fu D., Yang W., (2015), Magnetic nanoparticle clusters for photothermal therapy with near-infrared irradiation. *Biomater.* 39: 67-74.